ChemComm

Target identification of a macrocyclic hexaoxazole G-quadruplex ligand using a post-target-binding visualization

Journal:	*ChemComm*
Manuscript ID	CC-COM-07-2020-004957.R1
Article Type:	Communication

COMMUNICATION

Target identification of a macrocyclic hexaoxazole G-quadruplex ligand using a post-target-binding visualization

Received 00th January 20xx,
Accepted 00th January 20xx

DOI: 10.1039/x0xx00000x

Mizuho Yasuda,[a] Yue Ma,[b] Sachiko Okabe,[c] Yuki Wakabayashi,[a] Dongdong Su,[d] Young-Tae Chang,[e,f] Hiroyuki Seimiya,[c] Masayuki Tera,*[a] Kazuo Nagasawa*[a]

Macrocyclic hexaoxazoles (6OTDs) are G-quadruplex (G4) ligands, and some derivatives, such as L2H2-6OTD (1a) bearing two aminobutyl side chains, show cytotoxicity towards cancer cells. To identify the cellular target of 1a, we employed a post-target-binding strategy utilizing click reaction (Huisgen cyclization) between the azide-conjugated ligand L2H2-6OTD-Az (1b) and the cell-permeable dye CO-1 bearing a strained alkyne moiety and the BODPY fluorophore under Cu-free conditions. We confirmed that introduction of the small azide group did not alter the physical or biological properties, including anti-cancer activity, of 1a, and we also demonstrated bias-free localization of CO-1. The post-binding visualization strategy suggested that L2H2-6OTD (1a) colocalized with RNA G4 in living cells.

G-Quadruplexes (G4s) are stable, biologically important nucleic acid structures formed in consecutive guanine-rich sequences of gene promoter regions[1] and telomeres[2] in DNA, and in 3'- and 5'-untranslated regions in RNA.[1d,3] G4s in genomic DNA regulate basic biological events such as transcription,[4] replication,[5] and cellular senescence[6] with appropriate timings.[1e,7] On the other hand, G4s in RNA control translation in both untranslated[3c] and coding regions.[8] The RNA G4s are preferentially formed in single-stranded sequences,[9] when neither a complementary sequence competing with G4 nor a relevant chromatin structure is available. RNA G4s are thermodynamically more stable than DNA G4s,[10] and might therefore have a longer-lasting impact on cellular events than DNA G4s.

Numerous efforts have been made to develop G4 ligands as anti-cancer drug candidates.[7,11] For example, Neidle and co-workers have developed a series of naphthalene diimides as G4 ligands, and among them, CM03[11d] showed potent activity against several cancer cell lines *in vitro* and *in vivo*. CX-3543 developed by Hurley and co-workers exhibits anti-cancer activity by stabilizing G4 in rDNA, and was in a phase II clinical trial.[11a] However, high-throughput whole-genome sequencing indicates that at least 700,000 nucleic acid sequences can form G4 structure,[1b] and over 66,000 RNA G4s are predicted by calculation algorithms.[1d] Therefore, identification of the target G4s of G4 ligands in living cell, even to determine whether the target is DNA or RNA G4, is extremely challenging.

Some target identification studies have used fluorophore-conjugated derivatives of G4 ligands,[12,13] and the targets of carboxypyridostatin, QUMA-1 and ISCH-oa1, which show potent antiproliferative activity, were identified as RNA G4s. However, introducing a fluorophore into a small-molecular compound often drastically alters its biological and physical properties.[14] One approach to avoid this problem is a post target-binding visualization strategy, i.e., the introduction of a fluorophore into the compound of interest (COI) by means of a bioorthogonal reaction after the incubation of the COI into the cell. In this case, the physical and biological properties of COI should not be altered by its functionalization. For this purpose, Huisgen cycloaddition chemistry (click reaction), which involves reaction between azide and alkyne groups, has emerged as a promising strategy.[12c,15] In 2017, Teulade-Fichou and co-workers reported a pioneering study for the identification of the target of the G4 ligand Phen-DC3.[12c] They carried out the Huisgen cycloaddition reaction of alkyne-tagged Cy5 fluorophore with azido-modified Phen-DC3 under Cu-catalyzed and Cu-free conditions. However, different localization phenomena were observed depending on the presence or absence of copper; in particular, Cu-alkyne complex formation was associated with nucleolar localization of Phen-DC3. Thus, although they succeeded in visualizing intracellular Phen-DC3, there are still some questions

[a] *Department of Biotechnology and Life Science, Tokyo University of Agriculture and Technology, 2-24-16 Naka-cho, Koganei, Tokyo 184-8588 (Japan)*
E-mail: tera@go.tuat.ac.jp (M.T.), *knaga@cc.tuat.ac.jp* (K.N.)
[b] *Institute of Global Innovation Research, Tokyo University of Agriculture and Technology, 2-24-16 Naka-cho, Koganei, Tokyo 184-8588 (Japan)*
[c] *Division of Molecular Biotherapy, Cancer Chemotherapy Center, Japanese Foundation for Cancer Research, 3-8-1 Ariake, Koto-ward, Tokyo 135-8550 (Japan)*
[d] *Department of Chemistry and Chemical Engineering, Beijing University of Technology, Beijing 100124, China*
[e] *Center for Self-assembly and Complexity, Institute for Basic Science (IBS), Pohang 37673, Republic of Korea*
[f] *Department of Chemistry, Pohang University of Science and Technology (POSTECH), Pohang 37673, Republic of Korea*

† Electronic Supplementary Information (ESI) available: [details of any supplementary information available should be included here]. See DOI: 10.1039/x0xx00000x

regarding the difference in physical and biological properties between the COI and its azide-modified derivative, and the effects of using copper in the click reaction.

Here, we focused on Cu-free click reaction and selected a fluorescent dye exhibiting unbiased localization. We selected the azide group, one of the smallest bioorthogonal functional groups, for introduction into the G4 ligand to minimize the effect on its functional properties, and we chose CO-1 dye,[16] which is equipped with a strained alkyne moiety and the BODIPY fluorophore, as the reaction partner. Since CO-1 exhibits i) cellular permeability, ii) washability and iii) unbiased localization, it is expected to be suitable for *in situ* post-target-binding visualization with a low background in living cells. This strategy of using *in situ* click reaction chemistry between azide-modified G4 ligand **1a** (L2H2-6OTD-Az; **1b**) and fluorescent dye CO-1 for post-target-binding visualization enabled us to successfully identify the target molecule of **1a** in living cells (Figure 1).

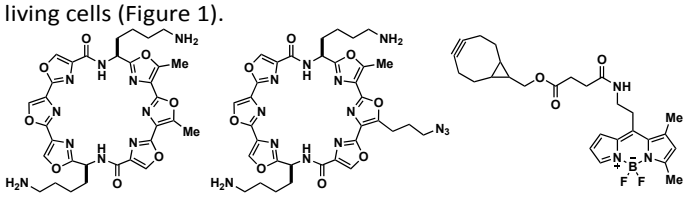

L2H2-6OTD (**1a**) L2H2-6OTD-Az (**1b**) CO-1

Figure 1. Structures of L2H2-6OTD (**1a**), L2H2-6OTD-Az (**1b**) and CO-1

We have developed a series of macrocyclic polyoxazole compounds as G4 ligands. Among them, heptaoxazole macrocycles (7OTDs) are efficient G4-specific probes *in vitro*, and have enabled the identification of thousands of G4s through either fluorescent polarization[17] or DNA microarray studies.[18] But, although our strategy with 7OTDs has been successful under cell-free conditions, it has some limitations for cellular imaging, mostly arising from the poor solubility of the structurally rigid 7OTDs under cell-compatible buffer conditions.[17] In contrast, in hexaoxazole compounds (6OTDs), the macrocyclic structure is more flexible, and modification of the two side chains in 6OTDs enables effective tuning of the solubility and physical properties. In particular, L2H2-6OTD (**1a**), which bears two aminobutyl side chains, has favorable physical properties, including solubility under conditions compatible with cell culture. In addition, the amino group in the side chain efficiently participates in the interaction with G4 through the cation-anion interaction with the phosphate backbone in the target G4, affording thermodynamically stable G4-L2H2-6OTD (**1a**) complex.[19] With this background in mind, we designed an azide-modified 6OTD ligand designated L2H2-6OTD-Az (**1b**).[20] The azide group is expected to undergo bioorthogonal click reaction with the strained alkyne group in CO-1, allowing the target to be fluorescently labelled in living cells.

At the outset, we examined the G4-stabilizing activity and biological properties of L2H2-6OTD (**1a**) and L2H2-6OTD-Az (**1b**) in both cell-free and cellular systems to assess whether or not introduction of the azide moiety affected the properties of **1a**. We examined the G4-stabilizing ability of **1a** and **1b** with G4-forming DNA (telo21), G4-forming RNA (TERRA), and double-stranded DNA (dsDNA, a negative control) by means of FRET melting analysis (Table 1).[21] While similar ΔT_m values of 20.0 ± 0.3 and 15.0 ± 0.1 against telo21, and 19.1 ± 0.2 and 17.3 ± 0.1 against TERRA were obtained for **1a** and **1b**, respectively, no ΔT_m change was observed with double-stranded DNA for either ligand (Figure S1). The G4-selective stabilization by **1a** and **1b** was maintained even in the presence of 100-fold excess of dsDNA as a competitor (Figure S1). Next, in the thiazole orange (TO) displacement assay with DNA G4,[22] displacement concentration values (DC_{50}) of 1.43 and 1.30 μM were obtained with **1a** and **1b**, respectively, indicating that both ligands bind at the G-quartet (Figure S2). RNA G4 displacement efficacy was also tested with ThT[23] in the presence of TERRA and the DC_{50} were measured as 297 and 213 nM for **1a** and **1b** (Figure S2). Thus, **1a** and **1b** show similar G4-stabilizing activity and binding mode, suggesting that introduction of the azide moiety has little effect on the properties of **1a**.

Oligonucleotides	ΔT_m values (°C)	
	1a	**1b**
telo21 (DNA)	20.0 ± 0.3	15.0 ± 0.1
TERRA (RNA)	19.1 ± 0.2	17.3 ± 0.2
Double-stranded DNA	0.0 ± 0.1	0.1 ± 0.1

Values are means of triplicate ± standard deviation.

Table 1. ΔT_m values of DNA or RNA telomeric G4 and double-stranded DNA in the presence of **1a** and **1b**.

We next examined the cytotoxicity of L2H2-6OTD-Az (**1b**) towards a panel of 16 cancer cell lines, including breast, CNS, colon, lung, melanoma, and stomach cells, in order to investigate the impact of its substituent group (azidoethyl group) on the biological activities.[24] After incubation with **1a** or **1b** for 48 h, the cell number was measured in terms of the total cell proteins (Figure 2). Compounds **1a** and **1b** showed very similar growth-inhibitory values (GI_{50}) in all of the cell lines examined. Furthermore, a plot of log GI_{50} of **1a** and **1b** showed a high correlation with an R^2 value of 0.96 and a slope of 0.99 (Figure S4). These results confirm that introduction of the azide propyl group has no significant effect on the properties of **1a**.

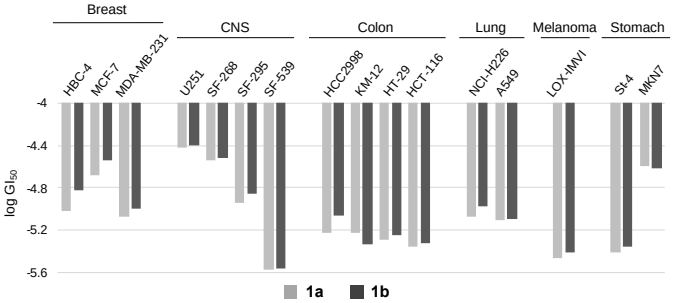

Figure 2. Growth-inhibitory activities of 6OTDs toward cancer cells. Growth-inhibitory effect of 6OTDs on a panel of 16 human cancer cell lines. Bars

represent log GI_{50} values for each cell line with **1a** (grey) and **1b** (black) after 48 h incubation.

Then, we attempted to identify the cellular target molecule of **1a** in fixed cells by utilizing the azide-modified probe **1b** and CO-1.[25] The cells were fixed with MeOH, and then treated with **1b** (10 μM) for 1 h, followed by addition of CO-1 (1 μM). After 1 h, nuclei were stained with DAPI and the fluorescence originating from CO-1 that had reacted with **1b** was measured. Fluorescence signals derived from CO-1 were detected in the cytoplasmic and nucleolar compartments. To obtain more insight into the nature of the target of **1b** in the cells, treatment with DNase or RNase was carried out before incubation of **1b** and CO-1 with U2OS cells. DNase treatment caused little change of the signals, whereas a significant reduction was observed after RNA digestion (Figure 3). This suggests that the target of **1a** is RNA, though this experiment did not establish whether **1b** was co-localized at RNA G4.

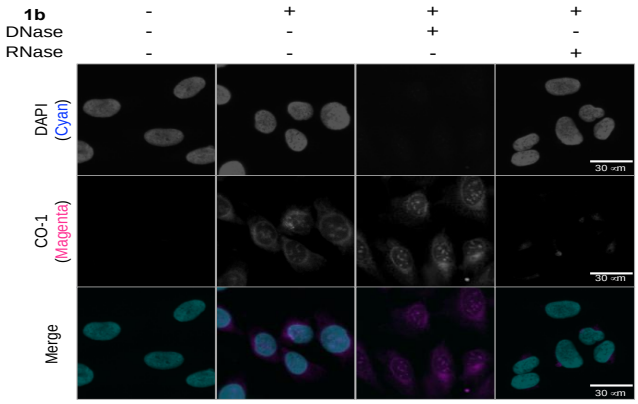

Figure 3. The click reaction of **1b** and CO-1 with fixed cells in the presence or absence of nuclease (DNase or RNase), and detection of fluorescence derived from CO-1.

To address this question, we conducted competitive binding experiments of **1b** with Phen-DC3, which is well known to bind to G4 specifically.[26] Thus, cells were pre-treated with Phen-DC3 to cover the G-quartet plane in G4, and then the same procedure for click reaction with **1b** and CO-1 was followed, as described above. Under these conditions, the fluorescence derived from CO-1 was concentration-dependently decreased by Phen-DC3, and it disappeared in the presence of 10 equivalents of Phen-DC3 with respect to **1b** (Figure S6). Moreover, the labelling efficacy of the target with **1b** and CO-1 was also decreased by post-treatment with Phen-DC3 (Figure S7). Overall, the results strongly imply that the target of **1b** is G4 contained in RNA.

Finally, we performed direct G4 staining with **1b** in living cells without any treatment (neither fixation nor permeabilization). Thus, U2OS cells were treated with **1b** (10 μM) for 24 h, in which no cytotoxicity was observed (Figure S5), washed with the medium, and then treated with CO-1 (300 nM) for 1 h to conduct the click reaction. The nuclei were stained with Hoechst33342. These cells contained fluorescent puncta, which were displaced by Phen-DC3 (Figure S8), suggesting the presence of RNA G4 targeted by **1b** in the cytoplasm (Figure 4).

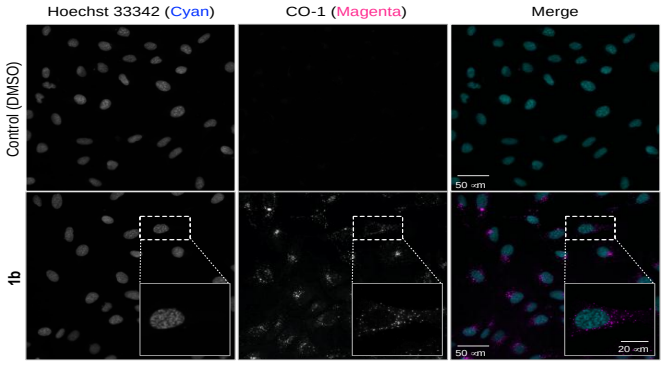

Figure 4. Fluorescence observed following the click chemistry between **1b** and CO-1 in the living U2OS cells.

Under these experimental conditions, only cytoplasmic but not nuclear foci were observed, suggesting that **1b** is readily incorporated into the cells across the plasma membrane, but remains in the cytoplasm. The observed foci were far too large to be single RNA molecules, and they may represent molecular complexes formed via co-assembly or condensation of RNAs (probably with RNA-binding proteins). One possibility might be stress granules, which are membrane-less organelles with high RNA contents, where G4 formation can potentially stall mRNA translation.[8b,27] Another possibility might be processing bodies (P-bodies), which contain rRNA.[28]

Conclusions

The target of the G4 ligand L2H2-6OTD (**1a**) was suggested to be RNA G4s in living cells by using a post-target-binding visualization strategy together with both in-cell Phen-DC3 displacement analyses and nuclease digestion assays. We confirmed that introduction of the azide moiety had little effect on the physical and biological properties of **1a**. The cellular permeability, washability, and bias-free localization of CO-1 make it an efficient tool for post-target-binding visualization of target molecules in living cells.

Conflicts of interest

There are no conflicts to declare.

Acknowledgements

This research was funded by Japan Society for the Promotion of Science (JSPS) (Scientific Research (B) 20H02876 to K.N.; (C) 19K05743 to M.T.; Early-Career Scientists 20K15411 to Y.M.), Grants-in-Aid for Scientific Research on Innovative Areas “Middle Molecular Strategy” (18H04387 to K.N.) and “Frontier Research on Chemical Communications” (20H04789 to H.S.), Japan Science and Technology Agency (JST) ACT-X JPMJAX191E to Y.M., Inamori Grants to M.T. and grants from the Nippon Foundation and The Translational Research program; Strategic PRomotion for practical application of INnovative medical Technology (TR-SPRINT) from the Japan Agency for Medical Research and Development to H.S. We thank the Molecular Profiling Committee, “Platform of Advanced Animal Model Support” (KAKENHI 16H06276) for JFCR39 and molecular

profiling analyses, and the international and interdisciplinary environment of the JSPS Asian CORE Program of ACBI.

Notes and references

1 (a) D. Rhodes and H. J. Lipps, *Nucl. Acids Res.*, 2015, **43**, 8627-8637; (b) V. S. Chambers, G. Marsico, J. M. Boutell, M. Di Antonio, G. P. Smith and S. Balasubramanian, *Nat. Biotech.*, 2015, **33**, 877-881; (c) J. L. Huppert and S. Balasubramanian, *Nucl. Acids Res*., 2005, **33**, 2908-2916; (d) J. L. Huppert, A. Bugaut, S. Kumari and S. Balasubramanian, *Nucl. Acids Res.*, 2008, **36**, 6260-6268; (e) A. K. Todd, M. Johnston and S. Neidle, *Nucl. Acids Res.*, 2005, **33**, 2901-2907.

2 (a) A. M. Zahler, J. R. Williamson, T. R. Cech and D. M. Prescott, *Nature*, 1991, **350**, 718-720; (b) S. Neidle, *FEBS J.*, 2010, **277**, 1118-1125; (c) L. Oganesian and T. M. Bryan, *Bioessays.*, 2007, **29**, 155-165; (d) J. Tang, Z. Y. Kan, Y. Yao, Q. Wang, Y. H. Hao and Z. Tan, *Nucl. Acids Res.*, 2008, **36**, 1200-1208; (e) Q. Wang, J. Q. Liu, Z. Chen, K. W. Zheng, C. Y. Chen, Y. H. Hao and Z. Tan, *Nucl. Acids Res.*, 2011, **39**, 6229-6237.

3 (a) D. Varshney, J. Spiegel, K. Zyner, D. Tannahill and S. Balasubramanian, *Nat. Rev. Mol. Cell Biol.*, 2020; (b) A. Arora and B. Suess, *Rna Biol.*, 2011, **8**, 802-805; (c) S. Kumari, A. Bugaut, J. L. Huppert and S. Balasubramanian, *Nat. Chem. Biol.*, 2007, **3**, 218-221.

4 A. Siddiqui-Jain, C. L. Grand, D. J. Bearss and L. H. Hurley, *Proc. Natl. Acad. Sci. U. S. A.*, 2002, **99**, 11593-11598.

5 Y. Kanoh, S. Matsumoto, R. Fukatsu, N. Kakusho, N. Kono, C. Renard-Guillet, K. Masuda, K. Iida, K. Nagasawa, K. Shirahige and H. Masai, *Nat. Struct. Mol. Biol.*, 2015, **22**, 889-897.

6 T. Miyazaki, Y. Pan, K. Joshi, D. Purohit, B. Hu, H. Demir, S. Mazumder, S. Okabe, T. Yamori, M. Viapiano, K. Shin-ya, H. Seimiya and I. Nakano, *Clin. Cancer Res.*, 2012, **18**, 1268-1280.

7 (a) J. Spiegel, S. Adhikari and S. Balasubramanian, *Trends Chem.*, 2020, **2**, 123-136; (b) H. Tateishi-Karimata and N. Sugimoto, *Chem. Commun.*, 2020, **56**, 2379-2390.

8 (a) T. Endoh, Y. Kawasaki and N. Sugimoto, *Nucl. Acids Res.*, 2013, **41**, 6222-6231; (b) T. Endoh, Y. Kawasaki and N. Sugimoto, *Angew. Chem. Int. Ed.*, 2013, **52**, 5522-5526.

9 (a) A. Arora and S. Maiti, *J. Phys. Chem. B*, 2009, **113**, 10515-10520; (b) M. M. Fay, S. M. Lyons and P. Ivanov, *J. Mol. Biol.*, 2017, **429**, 2127-2147.

10 P. Alberti and J. L. Mergny, *Proc. Natl. Acad. Sci. U. S. A.*, 2003, **100**, 1569-1573.

11 (a) D. Drygin, A. Siddiqui-Jain, S. O'Brien, M. Schwaebe, A. Lin, J. Bliesath, C. B. Ho, C. Proffitt, K. Trent, J. P. Whitten, J. K. C. Lim, D. Von Hoff, K. Anderes and W. G. Rice, *Cancer Res.*, 2009, **69**, 7653-7661; (b) C. L. Grand, H. Y. Han, R. M. Munoz, S. Weitman, D. D. Von Hoff, L. H. Hurley and D. J. Bearss, *Mol. Cancer Ther.*, 2002, **1**, 565-573; (c) M. H. Hu, T. Y. Wu, Q. Huang and G. Y. Jin, *Nucl. Acids Res.*, 2019, **47**, 10529-10542; (d) C. Marchetti, K. G. Zyner, S. A. Ohnmacht, M. Robson, S. M. Haider, J. P. Morton, G. Marsico, T. Vo, S. Laughlin-Toth, A. A. Ahmed, G. Di Vita, I. Pazitna, M. Gunaratnam, R. J. Besser, A. C. G. Andrade, S. Diocou, J. A. Pike, D. Tannahill, R. B. Pedley, T. R. J. Evans, W. D. Wilson, S. Balasubramanian and S. Neidle, *J. Med. Chem.*, 2018, **61**, 2500-2517; (e) T. Nakamura, S. Okabe, H. Yoshida, K. Iida, Y. Ma, S. Sasaki, T. Yamori, K. Shin-Ya, I. Nakano, K. Nagasawa and H. Seimiya, *Sci. Rep.*, 2017, **7**: 3605.

12 (a) G. Biffi, M. Di Antonio, D. Tannahill and S. Balasubramanian, *Nat. Chem.*, 2014, **6**, 75-80; (b) S. B. Chen, M. H. Hu, G. C. Liu, J. Wang, T. M. Ou, L. Q. Gu, Z. S. Huang and J. H. Tan, *J. Am. Chem. Soc.*, 2016, **138**, 10382-10385; (c) J. Lefebvre, C. Guetta, F. Poyer, F. Mahuteau-Betzer and M. P. Teulade-Fichou, *Angew. Chem. Int. Ed.*, 2017, **56**, 11365-11369; (d) X. C. Chen, S. B. Chen, J. Dai, J. H. Yuan, T. M. Ou, Z. S. Huang and J. H. Tan, *Angew. Chem. Int. Ed.*, 2018, **57**, 4702-4706; (e) E. Largy, A. Granzhan, F. Hamon, D. Verga and M. P. Teulade-Fichou, *Top. Curr. Chem.*, 2013, **330**, 111-177.

13 A few fluorescent G4 ligands are known, but in general, structural development of these compounds while retaining their fluorescence properties is difficult; see (a) A. Laguerre, K. Hukezalie, P. Winckler, F. Katranji, G. Chanteloup, M. Pirrotta, J. M. Perrier-Cornet, J. M. Y. Wong and D. Monchaud, *J. Am. Chem. Soc.*, 2015, **137**, 8521-8525; (b) X. Y. Luo, B. B. Xue, G. F. Feng, J. H. Zhang, B. Lin, P. Zeng, H. Y. Li, H. B. Yi, X. L. Zhang, H. Z. Zhu and Z. Nie, *J. Am. Chem. Soc.*, 2019, **141**, 5182-5191; (c) S. J. Xu, Q. Li, J. F. Xiang, Q. F. Yang, H. X. Sun, A. J. Guan, L. X. Wang, Y. Liu, L. J. Yu, Y. H. Shi, H. B. Chen and Y. L. Tang, *Nucl. Acids Res.*, 2015, **43**, 9575-9586.

14 (a) T. H. Zhao, X. L. Liu, S. Singh, X. S. Liu, Y. W. Zhang, J. Sawada, M. Komatsu and K. D. Belfield, *Bioconjug. Chem.*, 2019, **30**, 2312-2316; (b) J. Bucevicius, J. Keller-Findeisen, T. Gilat, S. W. Hell and G. Lukinavicius, *Chem. Sci.*, 2019, **10**, 1962-1970.

15 R. Rodriguez, K. M. Miller, J. V. Forment, C. R. Bradshaw, M. Nikan, S. Britton, T. Oelschlaegel, B. Xhemalce, S. Balasubramanian and S. P. Jackson, *Nat. Chem. Biol.*, 2012, **8**, 301-310.

16 S. H. Alamudi, R. Satapathy, J. Kim, D. D. Su, H. Y. Ren, R. Das, L. N. Hu, E. Alvarado-Martinez, J. Y. Lee, C. Hoppmann, E. Pena-Cabrera, H. H. Ha, H. S. Park, L. Wang and Y. T. Chang, *Nat. Commun.*, 2016, **7**: 11964.

17 M. Tera, K. Iida, K. Ikebukuro, H. Seimiya, K. Shin-ya and K. Nagasawa, *Org. Biomol. Chem.*, 2010, **8**, 2749-2755.

18 K. Iida, T. Nakamura, W. Yoshida, M. Tera, K. Nakabayashi, K. Hata, K. Ikebukuro and K. Nagasawa, *Angew. Chem. Int. Ed.*, 2013, **52**, 12052-12055.

19 (a) W. J. Chung, B. Heddi, M. Tera, K. Iida, K. Nagasawa and A. T. Phan, *J. Am. Chem. Soc.*, 2013, **135**, 13495-13501, (b) M. Tera, H. Ishizuka, M. Takagi, M. Suganuma, K. Shin-ya, K. Nagasawa, *Angew. Chem. Int. Ed*. 2008, **47**, 5557-5560, (c) Y. Kanoh, S. Matsumoto, R. Fukatsu, N. Kakusho, N. Kono, C. Renard-Guillet, K. Masuda, K. Iida, K. Nagasawa, K. Shirahige, H. Masai, *Nat. Struct. Mol. Biol.*, 2015, **22**, 889-897, (d) G. Mustafa, C. Chuang, W. Roy, M. Farhath, N. Pokhrel, Y. Ma, K. Nagasawa, E. Antony, M. Comstock, S. Basu, H. Balci, Biosens. Bioelectron., 2018, **121**, 34-40.

20 J. A. Punnoose, Y. Ma, M. E. Hoque, Y. X. Cui, S. Sasaki, A. H. Guo, K. Nagasawa and H. B. Mao, *Biochemistry*, 2018, **57**, 6946-6955.

21 A. De Cian, L. Guittat, M. Kaiser, B. Sacca, S. Amrane, A. Bourdoncle, P. Alberti, M. P. Teulade-Fichou, L. Lacroix and J. L. Mergny, *Methods*, 2007, **42**, 183-195.

22 (a) E. Largy, F. Hamon and M. P. Teulade-Fichou, *Anal. Bioanal. Chem.*, 2011, **400**, 3419-3427; (b) D. Monchaud, C. Allain and M. P. Teulade-Fichou, *Bioorg. Med. Chem. Lett.*, 2006, **16**, 4842-4845.

23 S. Xu, Q. Li, J. Xiang, Q. Yang, H. Sun, A. Guan, L. Wang, Y. Liu, L. Yu, Y. Shi, H. Chen and Y. Tang, *Sci. Rep.*, 2016, **6**, 24793.

24 T. Yamori, *Cancer Chemother. Pharmacol.*, 2003, **52**, S74-S79.

25 **1b** and CO-1 spontaneously were conjugated through the strain-promoted azide-alkyne cyclization (Figure S3).

26 A. De Cian, E. DeLemos, J. L. Mergny, M. P. Teulade-Fichou and D. Monchaud, *J. Am. Chem. Soc.*, 2007, **129**, 1856-1857.

27 S. Takahashi, K. T. Kim, P. Podbevsek, J. Plavec, B. H. Kim and N. Sugimoto, *J. Am. Chem. Soc.*, 2018, **140**, 5774-5783.

28 (a) S. G. Zhang, H. X. Sun, H. B. Chen, Q. Li, A. J. Guan, L. X. Wang, Y. H. Shi, S. J. Xu, M. R. Liu and Y. L. Tang, *Biochim. Biophys. Acta. Gen. Subj.*, 2018, **1862**, 1101-1106; (b) S. Mestre-Fos, P. I. Penev, S. Suttapitugsakul, M. Hu, C. Ito, A. S. Petrov, R. M. Wartell, R. Wu and L. D. Williams, *J. Mol. Biol.*, 2019, **431**, 1940-1955.

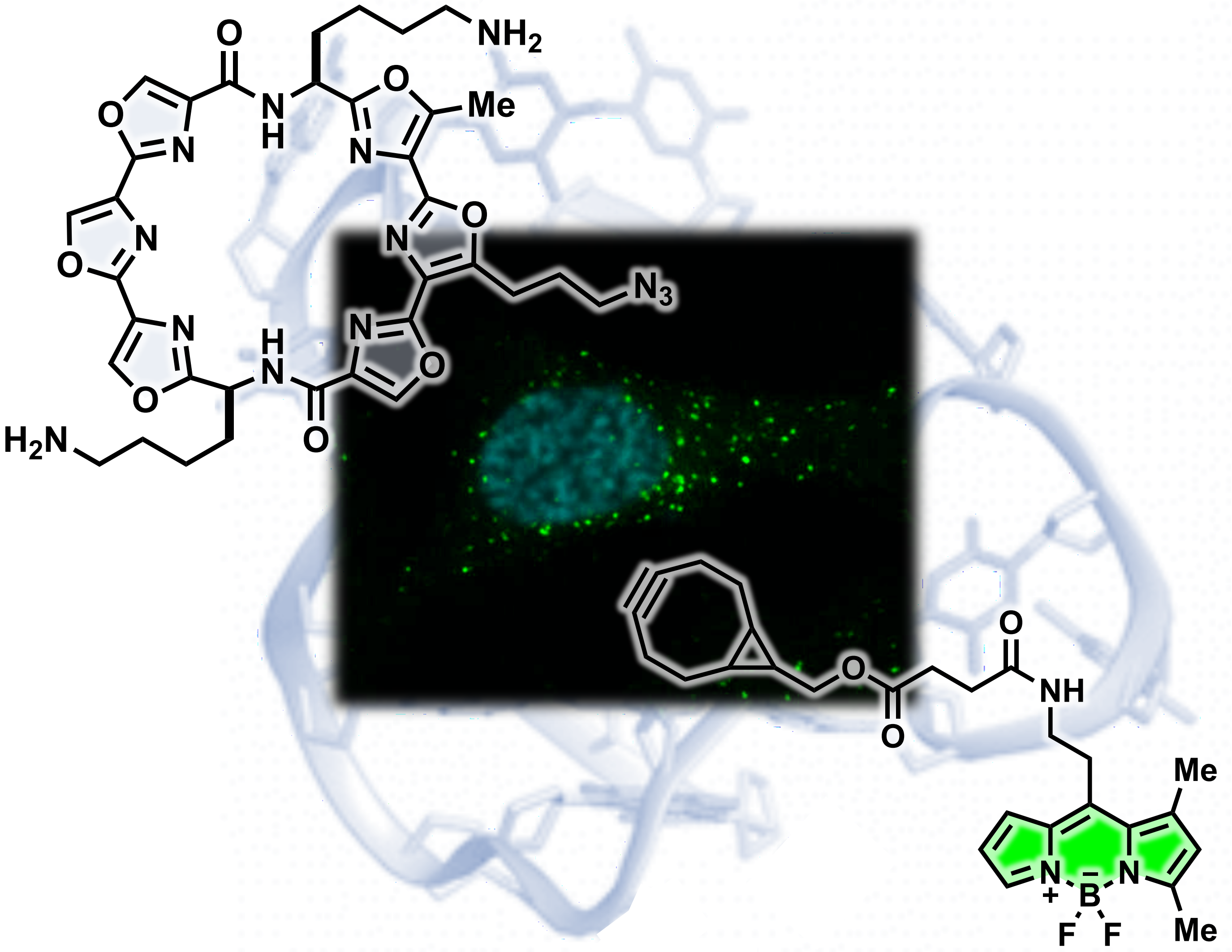
NH2
Me
N3
H2N
NH
Me
Me
F F